HIP-2017-09/TH

Prepared for submission to JCAP

Gravitational waves from non-Abelian gauge fields at a tachyonic transition

Anders Tranberg,[a] **Sara Tähtinen,**[b] **David J. Weir,**[b]

[a]Faculty of Science and Technology, University of Stavanger,
N-4036 Stavanger, Norway

[b]Department of Physics and Helsinki Institute of Physics,
P.O. Box 64, FI-00014 University of Helsinki, Finland

E-mail: anders.tranberg@uis.no, sara.tahtinen@helsinki.fi, david.weir@helsinki.fi

Abstract. We compute the gravitational wave spectrum from a tachyonic preheating transition of a Standard Model-like SU(2)-Higgs system. Tachyonic preheating involves exponentially growing IR modes, at scales as large as the horizon. Such a transition at the electroweak scale could be detectable by LISA, if these non-perturbatively large modes translate into non-linear dynamics sourcing gravitational waves. Through large-scale numerical simulations, we find that the spectrum of gravitational waves does not exhibit such IR features. Instead, we find two peaks corresponding to the Higgs and gauge field mass, respectively. We find that the gravitational wave production is reduced when adding non-Abelian gauge fields to a scalar-only theory, but increases when adding Abelian gauge fields. In particular, gauge fields suppress the gravitational wave spectrum in the IR. A tachyonic transition in the early Universe will therefore not be detectable by LISA, even if it involves non-Abelian gauge fields.

Keywords: cosmological phase transitions, physics of the early universe, primordial gravitational waves (theory)

Contents

1 Introduction

The ground-breaking direct detection of gravitational waves [1] gives promise that cosmological sources may also be detectable in the foreseeable future. One mission with scope to look for such sources is LISA, due for launch in 2034 [2]. The primary contenders for detection are gravitational waves from inflation (see for instance [3]), from cosmic defects (see for instance [4]) and from bubble collisions at a first order phase transition (see for instance [5]). The latter can in turn be connected to the creation of the cosmological baryon asymmetry if the phase transition in question is the electroweak one, at a temperature of around 100 GeV [6].

These processes are favoured observationally by LISA, because the scale of the dynamics is not primarily set by the microscopic properties of the system, such as particle masses. The long-wavelength behaviour of a system can play a significant role as well. For a first-order phase transition, this might correspond to the radius of bubbles of the new phase, which may grow to near-horizon scales. Similarly, cosmic strings potentially extend to the horizon and beyond and could give observable signals. In contrast, frequencies corresponding to electroweak mass-scales in the early Universe are much too high to be detectable by LISA, even when redshifted to the present epoch.

Another phenomenon with similar features arises when symmetry breaking is triggered at low temperature. Rather than a thermal phase transition, a spinodal (or tachyonic) decomposition occurs, whereby all momentum modes of the field with $|k|$ smaller than some mass scale μ grow exponentially in time. The UV effective cut-off μ is fixed by the microscopic physics of a given model, but the active IR part of the spectrum stretches all the way to $|\mathbf{k}| = 0$, or in a expanding Universe, to the Hubble scale. There is therefore hope that the large-amplitude momentum range in the associated gravitational wave spectrum may overlap with the one probed by LISA. We will investigate this here, for the case where the system includes non-Abelian gauge fields.

For all these different phenomena mentioned, numerical simulations are employed to compute the spectrum and strength of the gravitational wave signal. This is necessary, as the sources involve inhomogeneous, non-perturbative field dynamics [7–15]. Reheating at the end of inflation is typically modelled by one or more (self-)interacting scalar fields, which may or may not be coupled to gauge fields. For baryogenesis at a first order thermal phase transition, multiple fields are in play, but from the point of view of gravitational wave creation, these are likely well modelled by an ambient fluid, interacting with the Higgs field wall [9, 10, 16].

1.1 Tachyonic transitions

Spinodal decompositions are well-studied in condensed matter systems, but in a cosmological context, they are traditionally associated with hybrid inflation. This involves an inflation σ, coupled to a second scalar ϕ. As σ slow-rolls below a certain critical value, the effective mass parameter of the ϕ field becomes negative, and the transition is triggered. As a result, the slow-roll stage also ends, allowing for graceful exit from inflation.

But a tachyonic transition may arise in a wide variety of settings, as long as the dynamics of one field triggers the symmetry breaking of another, at low temperature. Examples of this include small- or large-field inflationary models, where slow-roll inflation has ended of its own accord, long before the symmetry breaking transition is triggered [17–19]; scenarios including spectator fields playing the role of σ, rolling from some non-zero initial condition set by the inflationary stage [20]; or indeed cases where the σ field is itself undergoing a symmetry breaking transition. There are also models where the scalar potential of a single field ϕ is such that a first order "tunnelling" occurs followed by tachyonic roll-down into the zero-temperature minimum [21, 22].

In the present work, we wish to investigate the IR properties of the gravitational wave (GW) spectrum from such a transition, and also to stay agnostic about the specific triggering mechanism and embedding in a UV theory. We will therefore model the quench in terms of a time-dependent mass. Writing for future convenience in terms of a complex scalar, we have for the second field ϕ

$$V(\phi) = V_0 + \mu^2_{\rm eff}(t)\phi^\dagger\phi + \lambda(\phi^\dagger\phi)^2, \tag{1.1}$$

where $\mu^2_{\rm eff}(t)$ is a model-dependent function of time (given by the motion of the inflaton or spectator field, or even of temperature). It is assumed to evolve from being positive to being negative, thereby triggering the symmetry breaking transition. We can model it as[1]

$$\mu^2_{\rm eff}(t) = \mu^2\left(1-\frac{2t}{\tau_q}\right), \qquad u = -\frac{1}{2\mu^3}\frac{d\mu^2_{\rm eff}(t)}{dt}\bigg|_{\mu_{\rm eff}=0} = \frac{1}{\mu\tau_q}, \tag{1.2}$$

with the understanding that the time dependence applies to the interval $0 \leq t \leq \tau_q$, and for $t > \tau_q$, $\mu_{\rm eff} = -\mu^2$. Matching to, for instance, a quartic "portal" coupling model $\xi^2\sigma^2\phi^\dagger\phi$, we could imagine writing

$$\mu^2_{\rm eff}(t) = (\xi^2\sigma^2 - \mu^2), \qquad u = -\frac{1}{2\mu^3}\frac{d\mu^2_{\rm eff}(t)}{dt}\bigg|_{\mu_{\rm eff}=0} = -\frac{\xi\dot\sigma_c}{\mu^2}, \tag{1.3}$$

so that $\tau_q \simeq -\mu/\xi\dot\sigma_c$, where the subscript c refers to the time of the quench $\sigma_c = \mu/\xi$.

[1] Our quench speed u is equivalent to the quantity V_c in [23].

Such a transition results in exponentially growing field modes with $|\mathbf{k}| \leq \mu$ [24]. The subsequent redistribution of the initial potential energy in V_0 is a highly effective preheating mechanism. In a given model, the additional kinetic energy of the σ field, and possible resonances (resonant preheating) must be considered (see for instance [25] in the context of baryogenesis).

The process of preheating through a spinodal transition is a violent and inhomogeneous process, and produces gravitational waves [23]. Even though the characteristic scales of the transition (typically μ and τ_q) are of the order of a GeV or more, and hence way beyond the sensitivity range of detectors such as LISA, the spectrum potentially extends in the IR to the scale of the horizon.

Previous simulations of scalar fields only [13, 15] have shown that gravitational waves are indeed produced in such a transition, but that the spectrum tends to peak around the scale of the particle masses. To the IR of this peak, there is first a $\propto k$ behaviour and then $\propto k^3$. This in spite of there being high occupation numbers in the field modes all the way to $k = 0$. For scalar fields, this is perhaps not unexpected given the form of the relevant source term (see below), but still disappointing. However, since these models are not directly connected to known physics (such as the Standard Model), there is some freedom in choosing the couplings and energy scale, including the quench speed u. In this way, one may construct models whose signal approaches the LISA-detectable region.

Whereas the σ field is often taken to be a gauge singlet, the second field ϕ need not be. Guided by the situation in the Standard Model, it is natural to expect both Abelian (U(1)) and non-Abelian (SU(N)) gauge fields to couple to such a "Higgs" field, and participate in the preheating mechanism [26, 27]. One may even entertain the notion that the second field *is* the Standard Model Higgs field. In this case, a fast spinodal transition from zero temperature, may be responsible for the baryon asymmetry of the Universe [28–31].

Reported investigations of GWs from tachyonic transitions in gauge-Higgs models consider the case where the gauge group is Abelian [7]. In that case the peak of the spectrum still stays in the UV, corresponding to the particle masses (scalar and gauge). Again, some freedom in the choice of parameters means it is possible to shift the peak amplitude and position towards the LISA detection region.

A crucial difference between the U(1)-Higgs and SU(2)-Higgs transitions is that in breaking the U(1) gauge symmetry, topological defects are created in the form of Abelian Higgs strings. A substantial literature exists on the late-time production of GWs from such networks of cosmic strings, including large-scale numerical simulations (see for instance the recent [32]). But also for short times, cosmic strings seem to give a contribution distinct from that due to the tachyonic dynamics itself [7].

Apart from it being a close analogue of the Standard Model, one upshot of investigating the SU(2)-Higgs model is that such topological defects are absent[2]. This allows us to focus on the GW-production from the spinodal growing IR modes themselves. Since non-Abelian fields self-interact strongly, such a contribution could a priori could be significant.

In the present work we will compute the spectrum of gravitational waves, as a function of the mass scale μ and the quench time τ_q. For most of our simulations, we will be conservative and assume a Standard Model-like theory, by setting the Higgs and gauge (self-)interaction couplings λ and g^2 equal to their Standard Model values. Hence, when the scale μ is around

[2]See however [33] for an analysis of transient local energy blobs related to "textures", "half-knots" and oscillons in that context.

100 GeV, our results apply directly to a Standard Model transition. When $\mu \gg 100$ GeV, the theory is a specific realisation of a generic SU(2)-Higgs system.

When appropriate, we will compare to a scalar-only theory as well as simulations of an Abelian U(1)-Higgs model. We stress again that such comparisons are sensitive to the presence of topological defects.

The paper is structured as follows. In the next Section, we will present our models, parametrisations and observables of interest. In Section 3 we set out our numerical procedure and definitions to compute the gravitational wave spectrum. In Section 4 we consider basic numerical observables, including components of the energy-momentum tensor, as well as the total energy generated in gravitational waves. We also present the full spectrum of gravitational waves, and analyse new features and contrast them with a scalar-only theory. We conclude in Section 5, where we also provide the extrapolation of the spectrum to the present day, and consider the potential for detection by LISA.

2 The SU(2)-scalar model

We consider a complex scalar doublet ϕ (four real components), coupled to an SU(2) gauge field A_μ. We have the action:

$$S_{4+G} = -\int d^4x \left\{ \frac{1}{4g^2} F^{a,\mu\nu} F_{a,\mu\nu} + \left[(D_\mu \phi)^\dagger D^\mu \phi + \mu^2_{\rm eff}(t) \phi^\dagger \phi + \lambda (\phi^\dagger \phi)^2 \right] \right\}, \tag{2.1}$$

where

$$F^a_{\mu\nu} = \partial_\mu A^a_\nu - \partial_\nu A^a_\mu + \epsilon^{abc} A^b_\mu A^c_\nu, \qquad D_\mu \phi = \left(\partial_\mu - i A^a_\mu \tau^a\right) \phi, \tag{2.2}$$

and $\mu^2_{\rm eff}(t)$ is given by Eq. (1.2). The scalar field components are

$$\phi = \frac{1}{\sqrt{2}} \begin{pmatrix} \phi_2 + i\phi_3 \\ \phi_0 + i\phi_1 \end{pmatrix}. \tag{2.3}$$

In the following, we will refer to the scalar as the Higgs field. Although we may only identify it with the Standard Model Higgs in the case where $\mu \simeq 100$ GeV, for any energy scale the symmetry breaking transition will lead to an analogue of the electroweak transition. In line with this terminology, we speak of the Higgs mass $m_H = \sqrt{2}\mu$, the Higgs expectation value $v = \mu/\sqrt{\lambda}$ and the W-mass (for the gauge fields), $m_W = gv/2$. We will take the Standard Model values from $m_H = 125$ GeV, $m_W = 80.2$ GeV, giving $\lambda \simeq 0.13$ and $g \simeq 0.65$. These we will keep fixed while varying μ^2 (and as a result, v). We will also briefly discuss varying λ (we consider $\lambda = 0.001$ and $\lambda = 0.01$), leaving the other parameters fixed. The lattice spacing will be fixed by $a\mu = 0.17$, with a lattice size of $N^3 = 384^3$ sites.

From the classical action (2.1), we can by variation with respect to ϕ and A_μ derive the classical equations of motion. These are explicit, coupled, non-linear, partial differential equations that can be solved by discretisation on a spatial cubic grid, and then evolved in time. We follow the standard procedure to do this (see, for instance [34]).

In a cosmological context, we should in principle include the expansion of the Universe through appropriately integrating the Friedmann-Robertson-Walker metric in the action. However, we know that the timescales involved are of the order of $10^2\mu^{-1}$, the total energy density is $V_0 = \mu^4/(4\lambda)$ and so we can ignore Hubble expansion as long as

$$1 \gg \frac{100H}{\mu} = 100\sqrt{\frac{1}{12\lambda}} \frac{\mu}{M_{\rm p}}. \tag{2.4}$$

Energy scales $\mu \lesssim 10^{13}$ GeV satisfy this bound for our choices of λ.

2.1 Reduced models

We are mainly investigating non-Abelian gauge-Higgs systems, but for comparison, we consider three other models, one with only a complex scalar field, one with a complex scalar field coupled to a U(1) gauge field and one with only a complex doublet[3], (essentially an O(4)-model). The actions are correspondingly for the complex singlet (denoted by the label "2")

$$S_2 = -\int d^4x \left[(\partial_\mu\phi)^*\partial^\mu\phi + \mu_{\rm eff}^2(t)\phi^*\phi + \lambda(\phi^*\phi)^2\right], \tag{2.5}$$

for the U(1)-complex singlet

$$S_{2+G} = -\int d^4x \left\{\frac{1}{4e^2}F^{\mu\nu}F_{\mu\nu} + \left[(D_\mu\phi)^*D^\mu\phi + \mu_{\rm eff}^2(t)\phi^*\phi + \lambda(\phi^*\phi)^2\right]\right\}, \tag{2.6}$$

where

$$F_{\mu\nu} = \partial_\mu A_\nu - \partial_\nu A_\mu, \qquad D_\mu\phi = (\partial_\mu - iA_\mu)\phi, \tag{2.7}$$

and for the complex doublet (denoted by the label "4"),

$$S_4 = -\int d^4x \left[(\partial_\mu\phi)^\dagger\partial^\mu\phi + \mu_{\rm eff}^2(t)\phi^\dagger\phi + \lambda(\phi^\dagger\phi)^2\right]. \tag{2.8}$$

Although in the following we describe the implementation and observables for the SU(2)-Higgs model (denoted by the label "4+G"), these all apply with trivial adaptations to the 2, 2+G and 4 case.

We note that with these standard conventions, the Higgs mass is always $m_H = \sqrt{2\lambda}v = \sqrt{2}\mu$, which we will keep the same for all models when comparing. On the other hand, whereas in the SU(2)-Higgs model the gauge field mass is $m_W = \frac{1}{2}gv$, in the U(1)-Higgs model, it is $m_W = ev$. When comparing, we will match the tree-level masses, and so take $e = g/2$.

2.2 Initial conditions

We will model the cold spinodal transition by assuming that the initial state is the vacuum in the potential

$$V_{\rm in}(\phi) = \mu^2\phi^\dagger\phi, \tag{2.9}$$

so that the (free) modes of the Higgs field obey

$$\left\langle\phi_a(k)\phi_b(k)^\dagger\right\rangle = \frac{1}{2\sqrt{\mu^2+k^2}}\delta_{ab}, \qquad \left\langle\pi_a(k)\pi_b(k)^\dagger\right\rangle = \frac{1}{2}\sqrt{\mu^2+k^2}\delta_{ab}. \tag{2.10}$$

with a denoting the four (two) real scalar degrees of freedom. We only initialise unstable modes with $|\mathbf{k}| < \mu$. These are the ones that grow large and subsequently validate the use

[3] Simulations with a single-component real field produce domain walls stretching through the lattice. This is interesting, but not relevant for us here.

of classical dynamics rather than full quantum dynamics. Careful discussions of this point can be found in Refs. [35–37]. Consistent with this way of thinking, all the gauge fields will be put to zero initially $A_\mu = 0$. Throughout, we will evolve the equations in temporal gauge $A_0 = 0$. We also initialise the gauge field conjugate momenta E_i to zero. There is therefore an insignificant residual per-site violation of the Gauss law of relative order 10^{-8}.

These initial conditions are closely related to those of Ref. [7]. However, we note that although one may classically scale out the vacuum expectation value v from the classical equations of motion for the scalar, one cannot in the same way rescale the quantum initial conditions. These are the same for any choice of v, provided μ is fixed. On the lattice they are determined by the choice of lattice scale. Hence, one may not trivially scale the results from one value of v to another, since the initial condition is then de facto different (although the resulting error is probably small). On the other hand, one may compute dimensionless ratios at a given lattice spacing (defined for instance in units of the mass $a\mu$), and then rescale trivially in μ. We will do this below.

2.3 Observables and Energy-Momentum tensor

The energy-momentum tensor of the theory follows from variation with respect to the metric. For the scalar field, we have for the energy density

$$\rho_\phi = (\partial_t\phi)^\dagger\partial_t\phi + (D_i\phi)^\dagger D_i\phi + \mu^2_{\text{eff}}(t)\phi^\dagger\phi + \lambda(\phi^\dagger\phi)^2 + V_0. \tag{2.11}$$

We may further subdivide this contribution into a kinetic (first term), gradient (second term) and potential part (the rest). Initially, the bulk of the energy is in V_0. An important consequence of our quench mechanism is that total energy is not conserved, because $\mu^2_{\text{eff}}(t)$ has an explicit time-dependence. We have that

$$\frac{dE}{dt} = \frac{d\mu^2_{\text{eff}}(t)}{dt}\int d^3\mathbf{x}\,\phi^\dagger\phi(\mathbf{x},t). \tag{2.12}$$

For the largest quench times presented here, this leads to a sizeable depletion of energy of up to 75%, or reduction of the final temperature of 50 %. This is the price we pay for simplifying the system by ignoring the specific and model-dependent dynamics of the trigger (inflaton) field.

It turns out [25] that such a quench, where energy is initially taken out of the Higgs field, corresponds to a particular parameter subspace of the model given in Eq. (1.3). At later times, energy is reintroduced as the system equipartitions and equilibrates. The time-scale for this to complete is much longer than the time-scales considered here. The late-time dynamics can also generate gravitational waves (see for instance [7]).

Gravitational waves are sourced by the off-diagonal spatial components T^ϕ_{ij}, given by

$$T^\phi_{ij} = (D_i\phi)^\dagger(D_j\phi) + (D_i\phi)(D_j\phi)^\dagger = 2\text{Re}\left[(D_i\phi)^\dagger(D_j\phi)\right]. \tag{2.13}$$

For the gauge field, we have

$$T^A_{\mu\nu} = \eta_{\mu\nu}\mathcal{L} - \frac{1}{g^2}\eta^{\alpha\beta}F^a_{\mu\alpha}F^a_{\nu\beta}. \tag{2.14}$$

The energy density is

$$\rho_A = \frac{1}{g^2}\left(F^a_{0\alpha}F^a_{0\alpha} + \frac{1}{4}F^{a,\mu\nu}F_{a,\mu\nu}\right) = \frac{1}{2}(E_i^2 + B_i^2). \tag{2.15}$$

The off-diagonal spatial components entering the gravitational wave computation are then

$$T^A_{ij} = -\frac{1}{g^2} F_i^{\beta,a} F^a_{j\beta}. \tag{2.16}$$

The complex singlet and doublet models for comparison have no gauge field contribution, and the scalar energy-momentum expressions include normal instead of covariant derivatives, with two and four real fields, respectively.

3 Gravitational wave production

Given the background scalar-gauge field theory simulation, from which we extract the energy-momentum tensor as described above, we can compute the gravitational wave spectrum as described in the following. For a more detailed exposition we refer to Ref. [10], and references therein. At each step of the simulation we compute the parts of the stress energy tensor that source metric perturbations, namely T^A_{ij} for the gauge field and T^ϕ_{ij} for the Higgs field. We can then numerically explicitly solve the wave equation for the metric perturbation u_{ij} [14],

$$\ddot{u}_{ij} - \nabla^2 u_{ij} = 16\pi G (T^\phi_{ij} + T^A_{ij}). \tag{3.1}$$

Going to momentum space

$$u_{ij}(\mathbf{k}) = \int d^3\mathbf{x}\, u_{ij}(\mathbf{x}) e^{-i\mathbf{k}\cdot\mathbf{x}}, \tag{3.2}$$

we can then project out the propagating, transverse-traceless degrees of freedom

$$h_{ij}(t,\mathbf{k}) = \lambda_{ij,lm}(\hat{\mathbf{k}}) u_{lm}(t,\mathbf{k}), \tag{3.3}$$

where

$$\lambda_{ij,lm}(\mathbf{k}) = P_{ik}(\mathbf{k})P_{jl}(\mathbf{k}) - \frac{1}{2}P_{ij}(\mathbf{k})P_{kl}(\mathbf{k}), \qquad P_{ij}(\mathbf{k}) = \delta_{ij} - \frac{k_i k_j}{|\mathbf{k}|^2}. \tag{3.4}$$

We can then construct the total energy density in the gravitational waves

$$\rho_{\mathrm{GW}} = \frac{1}{32\pi G V} \int \frac{d^3\mathbf{k}}{(2\pi)^3} \langle \dot{h}^{ij}(\mathbf{k}) \dot{h}^{ij}(-\mathbf{k}) \rangle, \tag{3.5}$$

where the average is to be taken over the full quantum state, or in practice an ensemble of realisations of the field theory initial conditions. Our ensembles of realisations are quite small, $\mathcal{O}(10)$ field configurations, since the convergence of the average turns out to be quite fast.

We may also define the spectrum of gravitational waves,

$$\frac{d\rho_{\mathrm{GW}}}{d\ln k} = \frac{1}{32\pi G V} \frac{k^3}{(2\pi)^3} \int d\Omega\, \langle \dot{h}^{ij}(\mathbf{k}) \dot{h}^{ij}(-\mathbf{k}) \rangle, \tag{3.6}$$

where the integral is now only over solid angle. The spectrum is then a function of the length of $\mathbf{k}$ only. Note the contraction of labels ij in Eqs. (3.5) and (3.6).

We solve Eq. (3.1) in parallel as the simulation of the (gauge-)Higgs system is performed. The source terms are time-dependent, and are in effect integrated over time to produce the final gravitational wave spectrum, and the total energy density in gravitational waves. This

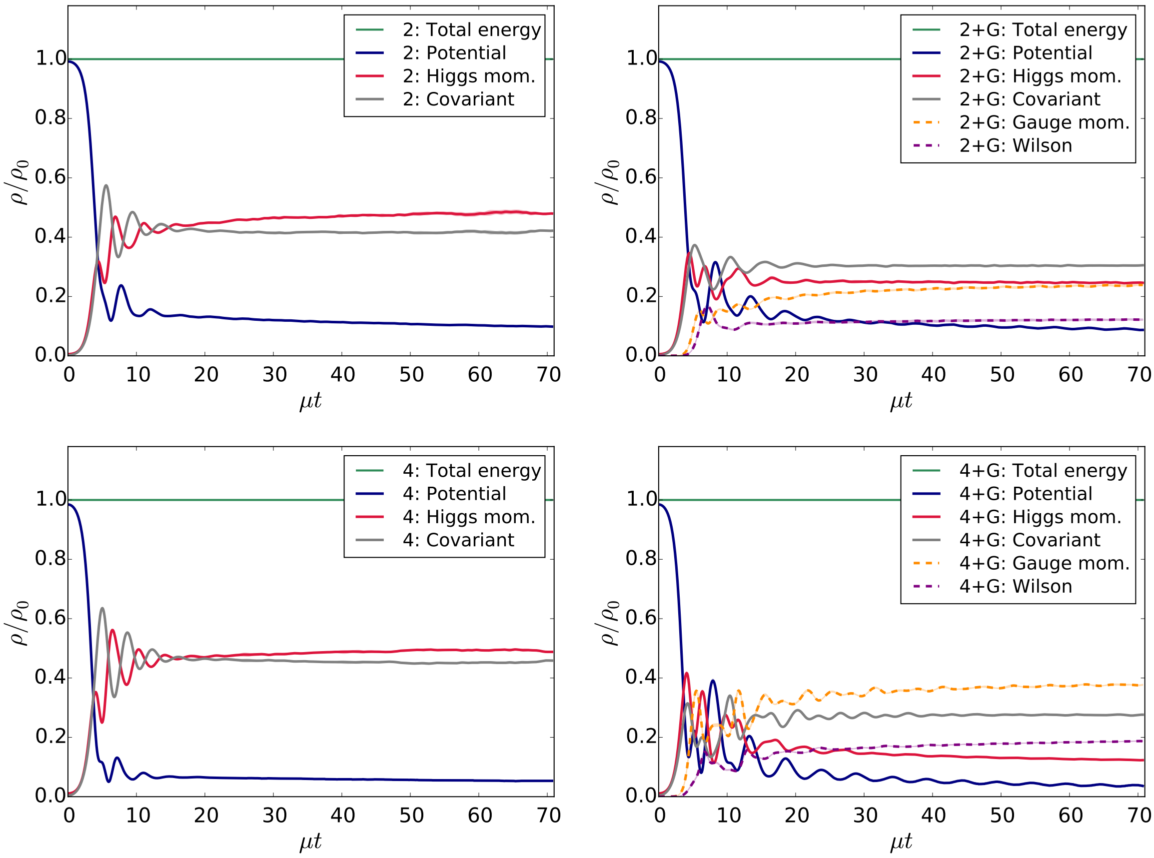

Figure 1. The energy components of the complex Higgs (top left), U(1)-Higgs (top right), doublet Higgs (bottom left) and SU(2)-Higgs (bottom right) systems. Quench time is $\mu\tau_q = 0$.

energy density is numerically completely negligible relative to the total energy density of the field theory system, and it makes little sense feeding the created gravitational waves back into the field theory simulation. Hence the gravitational waves are computed in the background of the (gauge-)Higgs system with no back-reaction. Ultimately, it is the quantity given by Eq. (3.6) that may be inferred from observations, suitably transported from the end of inflation to the present time. This is discussed further in Section 5.

4 Results

4.1 Energy distribution and total gravitational wave power

Gravitational waves are sourced by the off-diagonal components of the energy-momentum tensor, but it is instructive to consider the energy density and its components, to track where the energy goes. Initially, all the energy, except for small fluctuations in the Higgs field, is in the Higgs potential V_0. In a tachyonic transition, the low momentum modes $|\mathbf{k}| < \mu$ grow exponentially, picking up kinetic energy and gradient energy, while losing potential energy. With gauge fields coupled to ϕ, these will also grow exponentially, and reheat simultaneously [26].

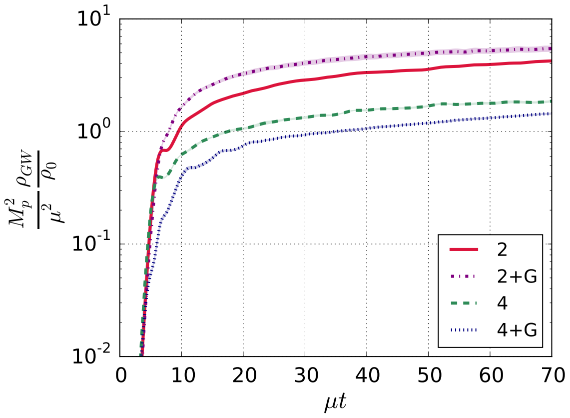

Figure 2. The total gravitational wave energy density for the four models under consideration, with $\mu\tau_q = 0$.

In Fig. 1, we show the various energy components for a simulation at one particular quench time $\mu\tau_q = 0$. In the top left panel, we show simulations with a complex scalar, top right when adding a U(1) gauge field. On the bottom left is the doublet scalar, bottom right when adding and SU(2) gauge field. We see that 80% of the potential energy is transferred to kinetic and gradient energy within $5\mu^{-1}$. There is some quantitative difference between the singlet and doublet case, but qualitatively they are very similar. The transition is over after $\mu t \simeq 15 - 20$. Note that for this case of zero quench time, no energy is lost because of the quenching process (2.12).

On the right-hand panels of the figure, we see that including the gauge field changes the situation. Although the potential energy is released very quickly as for the pure-scalar cases, this transfer only completes somewhat later. The Higgs field oscillates more and for longer and has a smaller fraction of the total energy. Some of this energy is instead transferred to the gauge field, which takes longer to be excited and settle, lasting until $\mu t \simeq 20 - 25$. There also seems to be a qualitative difference between U(1) and SU(2). For the Abelian gauge field, there is less energy in the gauge field than in the Higgs field (orange/purple compared to grey, red and blue). For SU(2), it is the other way around.

A detailed analysis of this preheating process in the SU(2)-Higgs model can be found in [26, 38]. The main features are that there is a short, violent roll-off period, followed by kinetic equilibration (and equipartition) as the self-interactions kick in, with a time-scale of a few hundreds in mass units. A Bose-Einstein-like particle spectrum is created with a sizeable effective chemical potential which disappears on a time-scale of a few thousands in mass units, through chemical equilibration.

We start by comparing the total energy density in gravitational waves for the four models under consideration in Figure 2. It is interesting to note that, whereas the addition of a U(1) gauge field increases the total gravitational wave energy density, the SU(2) gauge field suppresses it. This is an issue that we shall return to later.

In Fig. 3 (left), we show the total energy in gravitational waves from gauge-scalar simulations for five different quench times. The energy density is normalised to the initial energy in the Higgs potential, and with a prefactor $\mu^2/M_{\rm p}^2$, with $M_{\rm p}$ the Planck mass. For a given value of μ, one should therefore rescale the curves in the plot accordingly. As an example, the Standard Model has $\mu \simeq 88$ GeV, giving a prefactor of 1.3×10^{-33}.

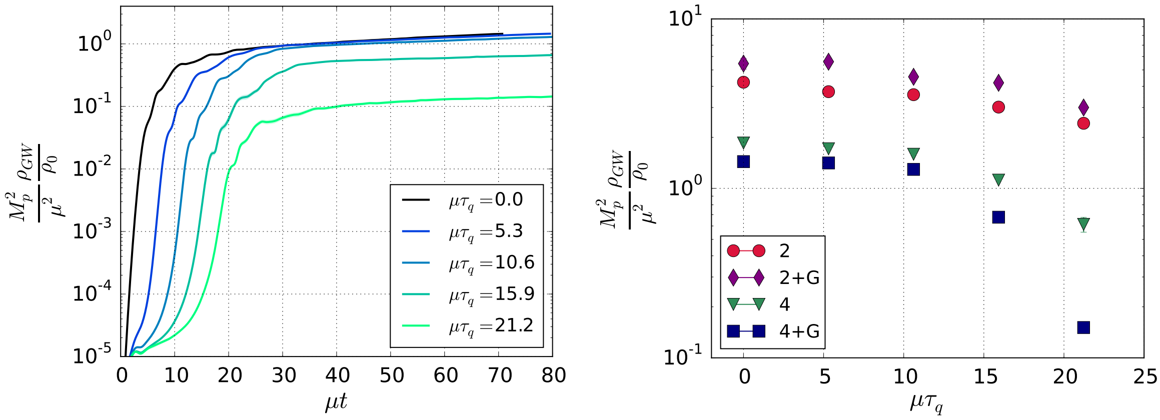

Figure 3. The total gravitational wave energy density for the SU(2)-Higgs model for five quench times (left). And the final value, for all quench times and models (right).

We see that the violent transition causes the gravitational energy to grow exponentially until a time $\mu t \simeq 10$ after the quench, and that it continues to grow slowly afterwards. We also see that the final total power at first has little dependence on quench time, and then decreases with quench time. This shows that when the time-scale of the quench is below a certain cut-off, the time-scale of the dynamics is the spinodal roll-off itself, rather than the quench time.

In Fig. 3 (right) we show the total gravitational wave energy for all four models, for all quench times. The total energy is independent of quench time for $\mu\tau_q > 10$, and then starts decreasing for slower quenches. Remarkably, the GW production increases when adding U(1) gauge fields to the complex scalar, whereas it decreases when adding SU(2) gauge fields to the doublet scalar (and more so for slower quenches). It seems that shifting energy into the self-interacting non-Abelian gauge field has the effect of reducing GW production.

4.2 Gravitational wave spectrum

Having found the total power in gravitational waves and its dependence on quench time, we now proceed to study in detail the power spectrum of gravitational waves produced by the transition. In Fig. 4, we show the spectra for different simulation times, fixing quench time $\mu\tau_q = 0$, for our four cases: a complex scalar (top left), when adding a U(1) gauge field (top right), for a doublet scalar (bottom left) and when adding and SU(2) gauge field to that (bottom right). We have again multiplied by a factor of $M_{\rm p}^2/\mu^2$, to be scaled back once a value for μ is chosen. The spectrum grows and converges in shape and magnitude at time $\mu t \simeq 60$.

For the scalar-only simulations, the spectrum is very similar, with a peak around $k/\mu = 0.7$ and an amplitude of about 1-2. The U(1)-Higgs spectrum has a bit more power in the UV. When adding gauge fields, the peak shifts to about $k/\mu = 1.4-1.6$, with the U(1)-Higgs peak becoming more pronounced. But whereas the U(1)-Higgs maximum is twice its scalar-only counterpart, for the SU(2)-Higgs model the amplitude does not change when adding gauge fields.

In Fig. 5 (left) we show the spectra at the final time of $\mu t = 70$. We again see the shift in peak position and amplitude when adding gauge fields. As the peak moves to the right, more of the IR-part of the spectrum is revealed, exhibiting a power law dependence.

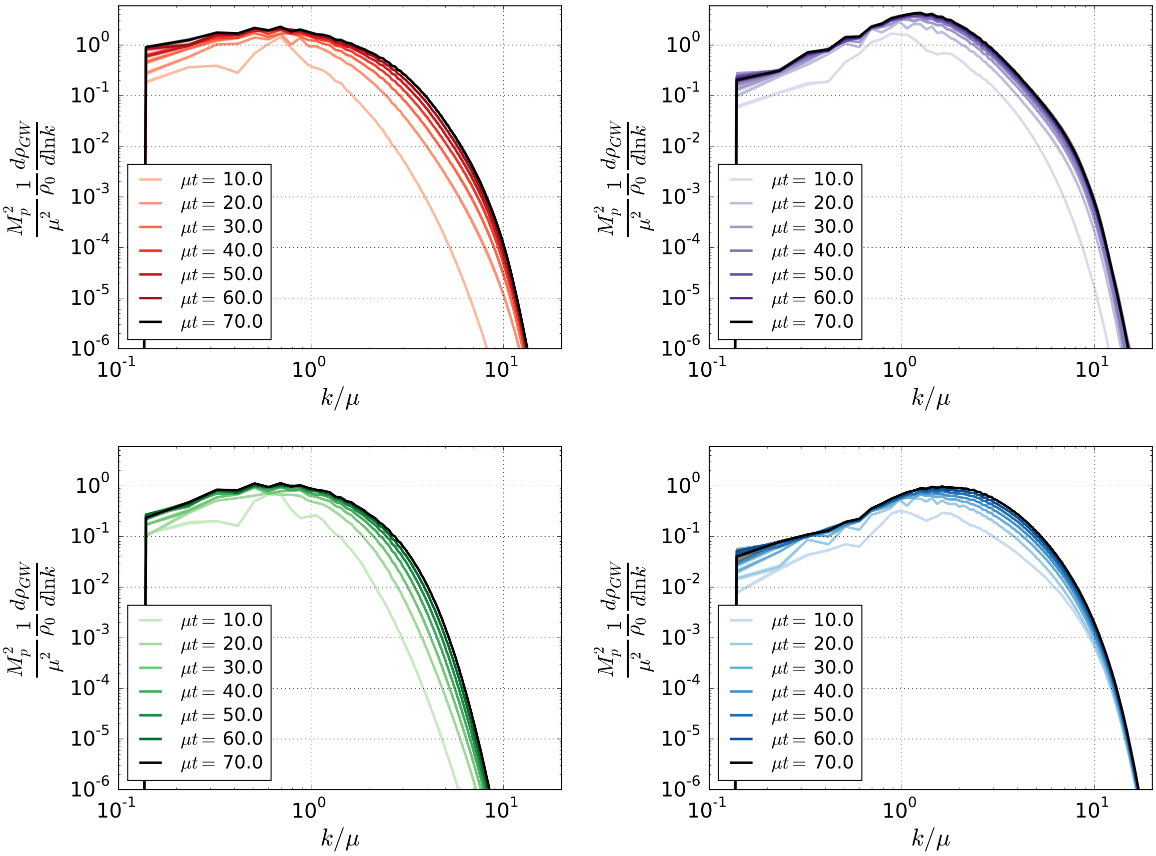

Figure 4. The power spectrum for different times, for the complex Higgs (top left), U(1)-Higgs (top right), doublet Higgs (bottom left) and SU(2)-Higgs (bottom right). Quench time is $\mu\tau_q = 0$.

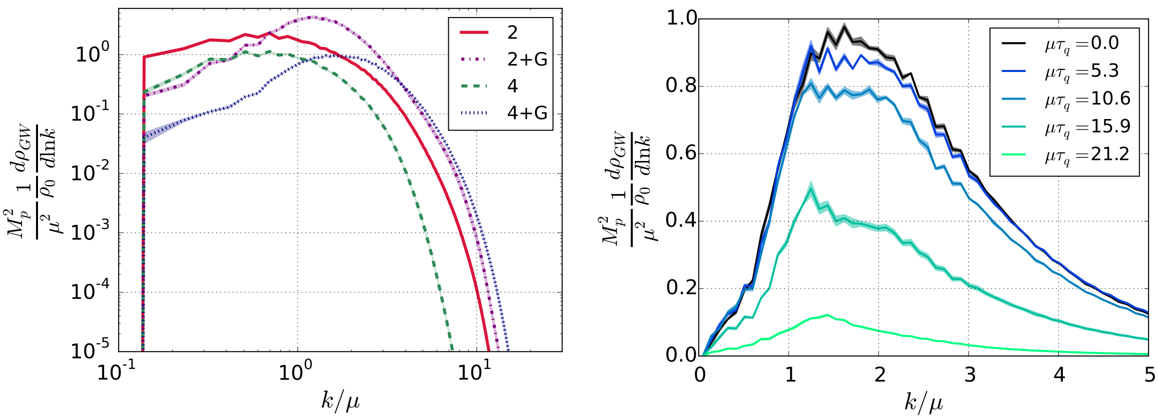

Figure 5. The final spectrum all four models (left). And for the SU(2)-Higgs case, for different quench times (right)

In the right-hand plot of the same figure, we then show the final spectrum for the gauge-doublet case for different quench times (this time on a linear scale). We see that the peak value decreases monotonically with longer quench time, although again the very

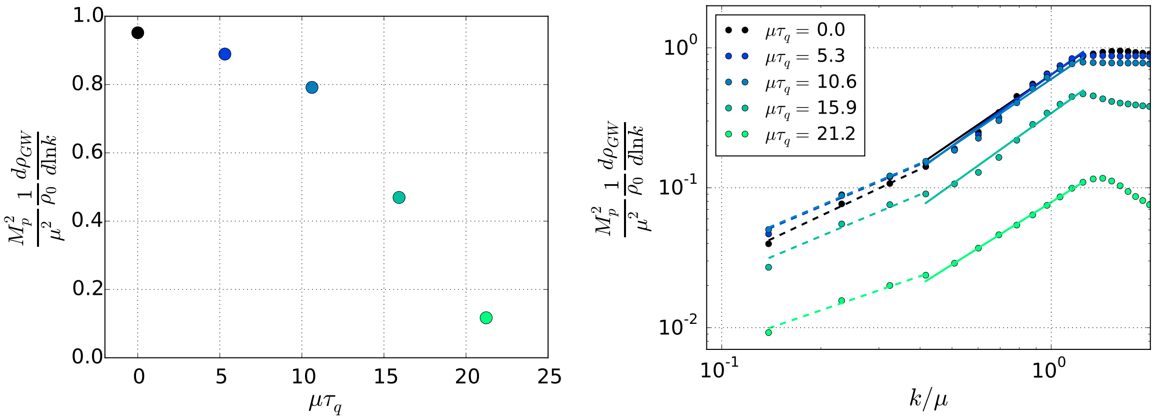

Figure 6. The peak amplitude (left) and IR slope (right) for different quench times. SU(2)-Higgs model only.

quick quenches cannot be resolved by the field dynamics. Note that since gravitational wave production continues in principle indefinitely, we have chosen to compare different quench time results at equal time after the end of the quench, $\mu t_{\rm final} = \mu\tau_q + 70$. The slowest quench has a peak amplitude down by a factor of 8.

Finally, we can attempt an analysis of the peak of the spectrum for the gauge-doublet case, shown in Fig. 6. The peak position varies in the range $k/\mu = 1.4 - 1.6$ (not shown). The peak amplitude (left-hand plot) shows a decreasing trend as a function of quench time, reminiscent of the total energy density in gravitational waves, Fig. 3. One may also attempt a fit of the IR slope(s) of the peak (right-hand plot) to find consistently a power of $1.5 - 1.75$ for all quench times on the range $\mu/2 < k < \mu$. However, this power law is replaced by a shallower $k-$dependence further in the IR, $k < \mu/2$. This far-IR power law is in the range $0.8 - 1.1$ and generally close to unity. Further still, at scales too large to study in our lattice simulations, this will give way to the causal k^3 power law.

4.3 Varying λ

So far, all our simulations have been done with $\lambda = 0.13$, the Standard Model value. The Standard Model is special in that the gauge boson and Higgs masses are very similar

$$\frac{m_H}{m_W} = \sqrt{\frac{8\lambda}{g^2}} \simeq 1.57. \tag{4.1}$$

This means that although there are two mass-scales in the problem (in addition to quench time), we only see one peak in the spectrum of gravitational waves.

One way to disentangle the two scales is to make λ (and hence m_H/m_W) smaller. We will keep μ fixed, and so what changes is m_W (in physical and lattice units) and the Higgs vev v. In Fig. 7 (left) we show the spectrum of gravitational waves for four different values of λ, for the gauge-scalar model only. We see that as the gauge boson mass increases (λ decreases) the peak resolves into two distinct peaks. The amplitude also increases significantly, by one or two orders of magnitude.

For $\lambda = 0.001$, the W-mass is clearly at the edge of our dynamical range ($am_W \simeq 7.3 \times am_H$), where lattice artefacts dominate, and we can therefore not go to even smaller

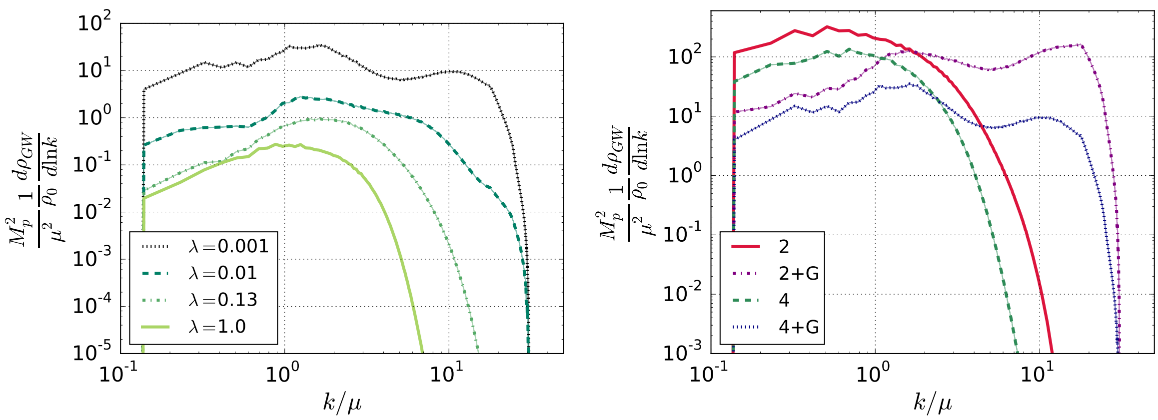

Figure 7. The SU(2)-Higgs spectrum for different λ (left), and for $\lambda = 0.001$ for all four models (right). $\mu\tau_q = 0$. Note the Brillouin zone edge at $k/\mu \approx 18.5$.

Higgs coupling. In order to confirm the origin of the second peak, we show in Fig. 7 (right) all four models with $\lambda = 0.001$. There is now no trace of the second peak, showing that the gauge field is the cause of it (and not, say, the value of v). The increase in magnitude as λ is decreased is common for all the models. For smaller λ, the exponential tachyonic instability lasts longer.

Such peak structure and other tell-tale features of multiple mass-scales would be possible targets for observations. However, the Higgs and W-mass scales are unfortunately far from the observational range of LISA. Tuning the parameters to shift the peaks into that range, although perhaps possible in principle, is not our main interest here.

5 Discussion and conclusion

As mentioned, we take the energy scale μ small enough relative to the Planck mass that we can ignore the expansion of the Universe during the time-scale of the simulation. Then we have the simple relation between a given physical scale on the lattice ak and the frequency f today [15]

$$f = 4 \times 10^{10}\ \mathrm{Hz}\left(\frac{ak}{a\rho^{1/4}}\right) = 4 \times 10^{10}\ \mathrm{Hz}\left(\frac{k}{\mu}\right)(4\lambda)^{1/4} = 3.4 \times 10^{10}\ \mathrm{Hz} \times \frac{k}{\mu}, \tag{5.1}$$

where we have taken the value $\lambda = 0.13$ (multiply by 0.3 for $\lambda = 0.001$). Hence, for fixed λ, the peak frequency for any choice of μ can be read off from the figures. Similarly, the amplitude of the spectrum is given by

$$\Omega_{\mathrm{gw}}h^2 = \frac{1}{\rho}\frac{d\rho_{\mathrm{GW}}}{d\ln k}\left(\frac{g_*}{g_0}\right)^{-1/3}\Omega_{\mathrm{rad}}h^2 = 9.3 \times 10^{-6} \times \frac{1}{\rho}\frac{d\rho_{\mathrm{GW}}}{d\ln k}, \tag{5.2}$$

using $\Omega_{\mathrm{rad}}h^2 = 4.3 \times 10^{-5}$ and $g_*/g_0 \simeq 100$. Again, this amplitude may therefore be read off from the figures, remembering to rescale by μ^2/M_{p}.

The peak sensitivity of the LISA mission is around 0.01 Hz, whereas our maximum signal occurs at $k/\mu \simeq 1.5$, corresponding to 5×10^{10} Hz. The peak amplitude is

$$\Omega_{\mathrm{gw}}h^2 = 9.3 \times 10^{-6}\left(\frac{\mu}{M_{\mathrm{p}}}\right)^2, \tag{5.3}$$

which is 10^{-38} for the electroweak scale and 10^{-12} for a GUT-scale transition. This applies to $\lambda = 0.13$, and we have seen that a few orders of magnitude can be gained by decreasing λ. Increasing the quench time decreases the magnitude of the gravitational spectrum, once the quench is slower than the finite time-scale off the Higgs roll-off.

When including gauge fields, we observe a stronger suppression in the IR (see also Ref. [7] for the Abelian case) with a power-law slope of about 1.6 near the peak. This gives way to a near-linear dependence further from the peak, although at very long wavelengths the causal behaviour of the source implies a steeper cubic power law. Hence, we expect that the signal 13 decades into the IR will be completely undetectable by LISA.

The most interesting effect of non-Abelian gauge fields is however, that the amplitude of GW decreases relative to a scalar-only theory. The opposite is the case for Abelian gauge fields. Most likely, this is an result of the non-Abelian self-interactions damping out the gauge-field sources of GW.

We saw that varying the coupling λ, a second peak corresponding to the gauge field mass emerges. It is possible that allowing for a very small (or zero) gauge field mass could overcome the IR suppression, by effectively shifting the gauge field peak far into the IR. The obvious candidate for this is the Standard Model photon but fields with very small masses are difficult to contain on a finite lattice. Also, although the identity of the photon is ambiguous during the tachyonic transition, once the Higgs mechanism is realised, the mass really is zero. There is no parameter with which to gradually "turn the mass off". We did not implement the photon in our simulations, and postpone a resolution of this issue to future work.

The peak signal frequency depends only on the scale μ through the combination k/μ, because we assume that the Hubble rate is determined by the Standard Model-inflaton energy component only. If another energy component than the Higgs potential would dominate the expansion of the Universe, the peak would redshift differently. Introducing such a new component, one would have to account for how it decays into SM degrees of freedom prior to BBN.

The hot plasma present in the early universe after reheating is an additional source of gravitational waves [39]. In fact, it might even prove to be a more significant source than the signal predicted for a tachyonic transition. The amplitude of gravitational waves from the plasma would be today (for typical Standard Model values of the energy density and shear viscosity)

$$\Omega_{\rm gw} h^2 \approx 10^{-6} \left(\frac{T_{\rm max}}{M_{\rm p}}\right) \tag{5.4}$$

where $T_{\rm max}$ would be the maximum temperature of the plasma, as it forms. This can be parametrically larger than the contribution of Eq. (5.3) by a factor $M_{\rm p} T_{\rm max}/\mu^2$, with a peak at wavenumber $k \sim T_0$, the temperature at which electroweak symmetry breaking takes place. This is in contrast to a first-order phase transition, where such plasma dynamics will be an insignificant source of gravitational waves except at the highest frequencies.

It is not a priori unreasonable to think that the copious production of particles in the IR would allow for detection of a tachyonic transition through gravitational waves. We have however seen that including non-Abelian gauge fields further suppresses the signal relative to scalar-only theories. With the possible caveats described above we must conclude that tachyonic preheating will not be observable at LISA.

Acknowledgments: AT is supported by a UiS-ToppForsk grant from the University of Stavanger. ST is supported by the Magnus Ehrnrooth foundation and Academy of Finland grant 267842. DJW is supported by Academy of Finland grant 267286. The authors thank Mark Hindmarsh for enlightening discussions. The numerical work was performed on the Abel Cluster, owned by the University of Oslo and the Norwegian metacenter for High Performance Computing (NOTUR), and operated by the Department for Research Computing at USIT, the University of Oslo IT-department.

References

[1] B. P. Abbott *et al.* [LIGO Scientific and Virgo Collaborations], Phys. Rev. Lett. **116** (2016) no.6, 061102 doi:10.1103/PhysRevLett.116.061102 [arXiv:1602.03837 [gr-qc]].

[2] H. Audley *et al.*, arXiv:1702.00786 [astro-ph.IM].

[3] N. Bartolo *et al.*, JCAP **1612** (2016) no.12, 026 doi:10.1088/1475-7516/2016/12/026 [arXiv:1610.06481 [astro-ph.CO]].

[4] P. Binetruy, A. Bohe, C. Caprini and J. F. Dufaux, JCAP **1206** (2012) 027 doi:10.1088/1475-7516/2012/06/027 [arXiv:1201.0983 [gr-qc]].

[5] C. Caprini *et al.*, JCAP **1604** (2016) no.04, 001 doi:10.1088/1475-7516/2016/04/001 [arXiv:1512.06239 [astro-ph.CO]].

[6] D. E. Morrissey and M. J. Ramsey-Musolf, New J. Phys. **14** (2012) 125003 doi:10.1088/1367-2630/14/12/125003 [arXiv:1206.2942 [hep-ph]].

[7] J. F. Dufaux, D. G. Figueroa and J. Garcia-Bellido, Phys. Rev. D **82** (2010) 083518 doi:10.1103/PhysRevD.82.083518 [arXiv:1006.0217 [astro-ph.CO]].

[8] D. G. Figueroa, M. Hindmarsh and J. Urrestilla, Phys. Rev. Lett. **110** (2013) no.10, 101302 doi:10.1103/PhysRevLett.110.101302 [arXiv:1212.5458 [astro-ph.CO]].

[9] M. Hindmarsh, S. J. Huber, K. Rummukainen and D. J. Weir, Phys. Rev. Lett. **112** (2014) 041301 doi:10.1103/PhysRevLett.112.041301 [arXiv:1304.2433 [hep-ph]].

[10] M. Hindmarsh, S. J. Huber, K. Rummukainen and D. J. Weir, Phys. Rev. D **92** (2015) no.12, 123009 doi:10.1103/PhysRevD.92.123009 [arXiv:1504.03291 [astro-ph.CO]].

[11] D. G. Figueroa, J. Garca-Bellido and F. Torrent, Phys. Rev. D **93** (2016) no.10, 103521 doi:10.1103/PhysRevD.93.103521 [arXiv:1602.03085 [astro-ph.CO]].

[12] M. Hindmarsh, S. J. Huber, K. Rummukainen and D. J. Weir, Phys. Rev. D **96** (2017) no.10, 103520 doi:10.1103/PhysRevD.96.103520 [arXiv:1704.05871 [astro-ph.CO]].

[13] J. Garcia-Bellido and D. G. Figueroa, Phys. Rev. Lett. **98** (2007) 061302 doi:10.1103/PhysRevLett.98.061302 [astro-ph/0701014].

[14] J. Garcia-Bellido, D. G. Figueroa and A. Sastre, Phys. Rev. D **77** (2008) 043517 doi:10.1103/PhysRevD.77.043517 [arXiv:0707.0839 [hep-ph]].

[15] J. F. Dufaux, A. Bergman, G. N. Felder, L. Kofman and J. P. Uzan, Phys. Rev. D **76** (2007) 123517 doi:10.1103/PhysRevD.76.123517 [arXiv:0707.0875 [astro-ph]].

[16] C. J. Hogan, Mon. Not. Roy. Astron. Soc. **218** (1986) 629.

[17] G. German, G. G. Ross and S. Sarkar, Nucl. Phys. B **608** (2001) 423 doi:10.1016/S0550-3213(01)00258-9 [hep-ph/0103243].

[18] B. J. W. van Tent, J. Smit and A. Tranberg, JCAP **0407** (2004) 003 doi:10.1088/1475-7516/2004/07/003 [hep-ph/0404128].

[19] G. G. Ross and G. German, Phys. Lett. B **691** (2010) 117 doi:10.1016/j.physletb.2010.06.017 [arXiv:1002.0029 [hep-ph]].

[20] K. Enqvist, P. Stephens, O. Taanila and A. Tranberg, JCAP **1009** (2010) 019 doi:10.1088/1475-7516/2010/09/019 [arXiv:1005.0752 [astro-ph.CO]].

[21] T. Konstandin and G. Servant, JCAP **1107** (2011) 024 doi:10.1088/1475-7516/2011/07/024 [arXiv:1104.4793 [hep-ph]].

[22] B. von Harling and G. Servant, JHEP **1801** (2018) 159 doi:10.1007/JHEP01(2018)159 [arXiv:1711.11554 [hep-ph]].

[23] J. F. Dufaux, G. Felder, L. Kofman and O. Navros, JCAP **0903** (2009) 001 doi:10.1088/1475-7516/2009/03/001 [arXiv:0812.2917 [astro-ph]].

[24] G. N. Felder, J. Garcia-Bellido, P. B. Greene, L. Kofman, A. D. Linde and I. Tkachev, Phys. Rev. Lett. **87** (2001) 011601 doi:10.1103/PhysRevLett.87.011601 [hep-ph/0012142].

[25] Z. G. Mou, P. M. Saffin and A. Tranberg, JHEP **1801** (2018) 103 doi:10.1007/JHEP01(2018)103 [arXiv:1711.04524 [hep-ph]].

[26] J. I. Skullerud, J. Smit and A. Tranberg, JHEP **0308** (2003) 045 doi:10.1088/1126-6708/2003/08/045 [hep-ph/0307094].

[27] K. D. Lozanov and M. A. Amin, JCAP **1606** (2016) no.06, 032 doi:10.1088/1475-7516/2016/06/032 [arXiv:1603.05663 [hep-ph]].

[28] J. Garcia-Bellido, D. Y. Grigoriev, A. Kusenko and M. E. Shaposhnikov, Phys. Rev. D **60** (1999) 123504 doi:10.1103/PhysRevD.60.123504 [hep-ph/9902449].

[29] L. M. Krauss and M. Trodden, Phys. Rev. Lett. **83** (1999) 1502 doi:10.1103/PhysRevLett.83.1502 [hep-ph/9902420].

[30] E. J. Copeland, D. Lyth, A. Rajantie and M. Trodden, Phys. Rev. D **64** (2001) 043506 doi:10.1103/PhysRevD.64.043506 [hep-ph/0103231].

[31] A. Tranberg and J. Smit, JHEP **0311** (2003) 016 doi:10.1088/1126-6708/2003/11/016 [hep-ph/0310342].

[32] M. Hindmarsh, J. Lizarraga, J. Urrestilla, D. Daverio and M. Kunz, Phys. Rev. D **96** (2017) no.2, 023525 doi:10.1103/PhysRevD.96.023525 [arXiv:1703.06696 [astro-ph.CO]].

[33] M. van der Meulen, D. Sexty, J. Smit and A. Tranberg, JHEP **0602** (2006) 029 doi:10.1088/1126-6708/2006/02/029 [hep-ph/0511080].

[34] K. Enqvist, S. Nurmi, S. Rusak and D. Weir, JCAP **1602** (2016) no.02, 057 doi:10.1088/1475-7516/2016/02/057 [arXiv:1506.06895 [astro-ph.CO]].

[35] J. Garcia-Bellido, M. Garcia Perez and A. Gonzalez-Arroyo, Phys. Rev. D **67** (2003) 103501 doi:10.1103/PhysRevD.67.103501 [hep-ph/0208228].

[36] J. Smit and A. Tranberg, JHEP **0212** (2002) 020 doi:10.1088/1126-6708/2002/12/020 [hep-ph/0211243].

[37] A. Arrizabalaga, J. Smit and A. Tranberg, JHEP **0410** (2004) 017 doi:10.1088/1126-6708/2004/10/017 [hep-ph/0409177].

[38] J. Garcia-Bellido, M. Garcia-Perez and A. Gonzalez-Arroyo, Phys. Rev. D **69** (2004) 023504 doi:10.1103/PhysRevD.69.023504 [hep-ph/0304285].

[39] J. Ghiglieri and M. Laine, JCAP **1507** (2015) no.07, 022 doi:10.1088/1475-7516/2015/07/022 [arXiv:1504.02569 [hep-ph]].